

FedX: Adaptive Model Decomposition and Quantization for IoT Federated Learning

*Phung Lai

University at Albany
Albany, New York, USA
lai@albany.edu

*Xiaopeng Jiang

Southern Illinois University
Carbondale, Illinois, USA
xiaopeng.jiang@siu.edu

An Chen, Vijaya Datta Mayyuri

Qualcomm Incorporated

San Diego, California, USA

anc@qualcomm.com, vmayyuri@qualcomm.com

NhatHai Phan, Cristian Borcea, Khang Tran

New Jersey Institute of Technology
Newark, New Jersey, USA

phan@njit.edu, borcea@njit.edu, kt36@njit.edu

Ruoming Jin

Kent State University
Kent, Ohio, USA
rjin1@kent.edu

Abstract—Federated Learning (FL) allows collaborative training among multiple devices without data sharing, thus enabling privacy-sensitive applications on mobile or Internet of Things (IoT) devices, such as mobile health and asset tracking. However, designing an FL system with good model utility that works with low computation/communication overhead on heterogeneous, resource-constrained mobile/IoT devices is challenging. To address this problem, this paper proposes FedX, a novel adaptive model decomposition and quantization FL system for IoT. To balance utility with resource constraints on IoT devices, FedX decomposes a global FL model into different sub-networks with adaptive numbers of quantized bits for different devices. The key idea is that a device with fewer resources receives a smaller sub-network for lower overhead but utilizes a larger number of quantized bits for higher model utility, and vice versa. The quantization operations in FedX are done at the server to reduce the computational load on devices. FedX iteratively minimizes the losses in the devices’ local data and in the server’s public data using quantized sub-networks under a regularization term, and thus it maximizes the benefits of combining FL with model quantization through knowledge sharing among the server and devices in a cost-effective training process. Extensive experiments show that FedX significantly improves quantization times by up to $8.43\times$, on-device computation time by $1.5\times$, and total end-to-end training time by $1.36\times$, compared with baseline FL systems. We guarantee the global model convergence theoretically and validate local model convergence empirically, highlighting FedX’s optimization efficiency.

Index Terms—Federated learning, Heterogeneous IoT, Model decomposition, Quantization.

I. INTRODUCTION

In Federated Learning (FL), a global model is trained by aggregating local model’s gradients across devices, while ensuring user privacy by not sharing local data [1]. This feature makes FL suitable for building intelligent mobile/IoT systems and enhancing model generalization/utility, compared with individual local models. Examples include mobile health, where users employ heterogeneous IoT devices (i.e., phone, smart watches, mHealth sensors) to monitor health information and

human activities [2], and fleet tracking, where businesses use different IoT devices to track assets or vehicles [3]. In these systems, the devices exhibit heterogeneity, but collaborate to achieve the same system goals by performing identical tasks.

The hardware heterogeneity of IoT devices in terms of computation, communication, and storage raises a main challenge for FL systems: How to balance model utility with computation and communication overhead, given heterogeneous and limited on-device resources? Achieving high model utility may require resource-intensive models and multi-round communication, straining resource-constrained devices. Large models can be too slow, difficult to execute, or consume too much battery power, while small models on all devices may overlook that some devices can handle the larger models that perform better.

Model compression and distillation address computation and communication overhead on resource-constrained devices. Quantization-based compression approaches [4], [5] reduce communication load by reducing parameter or gradient precision. Other compression methods are sparsification, pruning, reduction, and sampling [6], [7]. However, these techniques often sacrifice utility or focus on communication reduction at the expense of computation. In model distillation [8], different devices with heterogeneous resources initially train their model using public data, then retrain locally using their private data. To mitigate the reliance on public data, some works [9], [10] leverage quantization on devices and conduct model shrinking or knowledge distillation to align utility of the local model with that of the global model. While effective, these techniques can impose significant computational overhead on clients. In addition, knowledge distillation, tiering, and split learning-based FL [8], [11], [12] focus on individual devices without globally balancing utility, computation, and communication. Therefore, there is a crucial need for an efficient and effective FL for heterogeneous and resource-constrained IoT devices.

§* Equal contribution

Contributions. This paper proposes **FedX**, an adaptive model decomposition and quantization FL system for IoT. To balance model utility with resource constraints on IoT devices, FedX decomposes a global FL model into different sub-networks with different quantization levels for different devices. The key idea to achieve this balance is that a device with fewer resources receives a smaller sub-network for lower overhead, but utilizes a larger number of quantized bits for higher model utility, and vice-versa. The sub-networks used by the devices are nested within each other; that is, a smaller sub-network is always contained inside a larger sub-network. This approach fosters knowledge sharing among IoT devices, since on-device training and updating any sub-network will improve other sub-networks through the model aggregation in the federated training. Quantization operations in FedX are done at the server to reduce the computation load on IoT devices, notably without affecting their model utility.

FedX starts from a global model trained on publicly available data and fine-tunes it to align it with the local data distributions of IoT devices, which frequently differ from the global model's distribution. During this process, reducing the disparity between the global models before and after fine-tuning is crucial to ensure that the fine-tuned global model effectively learns the distinctive distribution present in the server's data while retaining the knowledge acquired from the data distributions of the IoT devices. To ensure minimal disparity between the global models before and after fine-tuning, we add a regularization minimizing the difference between the global models during fine-tuning. The features of FedX maximize the benefits of combining FL with model quantization by enabling knowledge sharing among the server and the devices in a cost-effective training process.

Extensive experiments on image classification and human activity recognition show that FedX outperforms state-of-the-art adaptive quantization approaches for FL [4], [10] by 1.90% – 12.28% in accuracy. In addition, using NVidia Jetson Nano, Qualcomm QCS605 AI kit, and Raspberry Pi 5, FedX shows significant improvement in quantization time by $8.43\times$, on-device computation time by $1.5\times$, and total end-to-end training time by $1.36\times$, compared with baseline FL systems.

II. BACKGROUND

A. Federated Learning

Federated Learning (FL) is a multi-round protocol where a server sends a global model θ^t to a random subset of M^t devices at each training round t . These devices train the model locally and send updates back. The server aggregates the updates using a function $\mathcal{G} : R^{|M^t| \times n} \rightarrow R^n$ (n is the size of θ^t), producing the aggregated model $\theta^{t+1} = \mathcal{G}(\{\theta_u^{t+1}\}_{u \in M^t})$. FedAvg is a common aggregation method in FL [13].

B. Quantization-based Compression

Quantization-based compression approaches in FL typically speeds up model convergence and minimizes communication

[5], [10], [14]. In FedX, we consider stochastic fixed-point quantization, i.e., QSGD [4], [14]. The quantization function, denoted as $\mathbb{Q}(\cdot, q)$ with $q \geq 1$, represents quantized bits, corresponding to the number of bits used for each value. Technically, q is associated with 2^q levels of quantization. Each value is quantized in a manner that maintains its expected value while minimizing variance. The quantizer $\mathbb{Q}(\theta, q)$ quantizes the vector θ element-wise, returning the sign of θ and $\|\theta\|_2$ rounded to one of the endpoints of its encompassing interval.

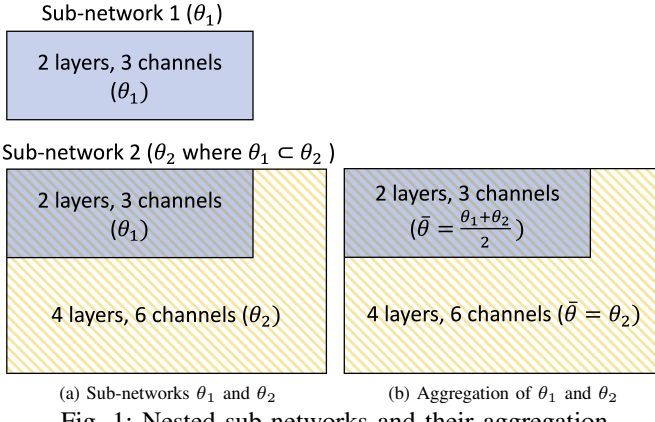
QSGD quantizes θ in three steps: 1) Quantize θ as $\mathbb{Q}(\frac{\theta}{\|\theta\|_2})$ into 2^q bins in $[0, 1]$, storing signs and $\|\theta\|_2$ separately; 2) Encode the results with 0 run-length encoding; and 3) Encode the results with Elias ω coding. The first step is a lossy transformation, where a higher q lowers the loss, while subsequent steps are lossless. These steps reduce device computation and communication bits, including distributing updated models between the server and devices and sending parameter/gradient updates. Quantization further reduces device computation by using fewer bits to represent values.

III. FEDX: AN ADAPTIVE QUANTIZATION FL SYSTEM

FedX Settings and Objectives. We consider a setting in which the server's collected data D_S and devices' local data $\{D_u\}_{u \in [1, N]}$ are complementary to each other but may not be in the same or similar distribution. For instance, in asset tracking, devices can leverage local data to recognize more specialized and diverse objects than the server's public data. The server and all the devices u jointly train an aggregated global model θ and the devices' local models $\{\theta_u\}_{u \in [1, N]}$, such that the global and local models can recognize objects from both the client data and the server data after federated training. This configuration is practical as the server can access public data, which can supplement, but differ from the on-device data collected from various devices.

In this setting, FedX aims to enhance FL for heterogeneous IoT devices with adaptive decomposition and quantization, addressing: (i) device-tailored models balancing utility with resource constraints and overhead; (ii) adaptive quantization during training; (iii) low overhead on-device training; and (iv) computation savings at inference. This approach improves model utility and system effectiveness while reducing training, quantization, and inference overhead. Key challenges are: (1) balancing model utility with computation/communication overhead from device heterogeneity, and (2) optimizing knowledge transfer to reduce performance disparity and improve utility.

To address these challenges, departing from existing FL systems, the key idea of FedX is to decompose the global model θ into smaller sub-networks $\theta_u \subseteq \theta$ (Fig. 1), each tailored to a device's resources. Devices with fewer resources receive smaller sub-networks for lower training overhead, while using more quantized bits for higher utility and efficient inference; and vice-versa. These local sub-networks are aggregated to update the global model $\theta = \mathcal{G}(\theta_{u \in [1, N]})$.



(a) Sub-networks θ_1 and θ_2

(b) Aggregation of θ_1 and θ_2

Fig. 1: Nested sub-networks and their aggregation.

The optimization function for global and local models is:

$$\theta^* = \arg \min_{\theta} \left[\sum_{u \in [1, N]} \mathcal{L}(\mathbb{Q}(\theta_u, q_u), D_u) + \mathcal{L}(\theta, D_S) \right]$$

s.t. $\forall u \in [1, N] : \theta_u \subseteq \theta$ and $\theta = \mathcal{G}(\{\theta_u\}_{u \in [1, N]})$, (1)

where \mathcal{L} is a loss function and \mathbb{Q} is a quantization function, such as QSGD, with the numbers of quantized bits $\{q_u\}_{u \in N}$ and the local model $\{\theta_u\}_{u \in N}$ tailored to the device u . The first term $\sum_{u \in [1, N]} \mathcal{L}(\mathbb{Q}(\theta_u, q_u), D_u)$ is the loss across devices given quantized local models $\mathbb{Q}(\theta_u, q_u)$ on their local model θ_u and data D_u ; the second term $\mathcal{L}(\theta, D_S)$ is the loss of the aggregated global model θ on the server's data D_S .

In practice, the number of device types (as a function of their resource capabilities) is expected to be small; thus, instead of individual devices, we can consider categories of devices (similar amount of resources) that have the same sub-network or number of quantized bits without affecting the generality of our objectives. Also, we do not consider a weighted correlation between the two losses since the server and the devices can optimize them independently in our training protocol.

A. Adaptive Model Decomposition and Quantization

In FedX, the server decomposes θ into a suitable sub-network θ_u and identifies a suitable number of quantized bits to each device u based on its resources. Given θ , the potential sub-networks can be exponentially large. Some may fail to perform well or hinder knowledge sharing among devices, especially if they occupy different parts of the global model.

To address this problem, the server generates and trains a small set of sub-networks using its publicly available data D_S . In FedX, a smaller sub-network is always contained inside a larger sub-network. We call this setting **nested sub-networks**. For instance, we consider the two sub-networks θ_1 and θ_2 (Fig. 1a). The sub-network θ_1 has 2 layers, each of which has 3 channels. The sub-network θ_2 has 4 layers, each of which has 6 channels. The sub-network θ_1 is a subset of model parameters given the sub-network θ_2 such as $\theta_1 \subset \theta_2$.

For instance, in our experiments with images, we use CompOFA [15] with MobileNetV3 [16] as the global model

θ . CompOFA is a centralized training approach to generate and train sub-networks with varying sizes from a larger model for efficient IoT deployment, reducing potential sub-networks while maintaining utility. The server generates 243 nested sub-networks ranging from 2.41M to 6.39M parameters, achieving good utility on server data D_S . However, due to differing data distributions between devices and the server, these sub-networks may not perform well on devices' data $D_{u \in [1, N]}$ before federated training. This nested sub-network approach generalizes beyond CompOFA and MobileNetV3, as demonstrated in our human activity recognition experiments.

Using a small set of nested sub-networks as local models θ_u enables effective knowledge sharing among IoT devices, as updates in any sub-network benefit others during federated training. Our observations indicate that failure to construct these nested sub-networks significantly damages model utility, as non-nested updates from different clients can cause misalignment among them. While neural architecture search can yield high-accuracy and efficient architectures [17], it requires repeating the search process and retraining for new hardware platforms, limiting scalability. In addition, individually trained models with no shared weights result in a large total model size that requires high download bandwidth requirements [18].

To select a suitable sub-network and identify the quantized bits for device u , we use the following metrics and process:

Selection Metrics. 1) *Utility Drop*: This is the difference in prediction accuracy between the global model and a particular (either original or quantized) sub-network. 2) *On-device Training Time*: It is the training time per local round on a device using a sub-network.

Although a sub-network can have efficient on-device training time, quantization¹ may significantly degenerate its model utility. Hence, a suitable sub-network θ_u for a device u must balance the trade-off between performance drop, on-device training time, and the number of quantized bits q_u . We formulate this trade-off as follows:

$$\begin{aligned} \theta_u, q_u = \arg \min_{\theta_u \in \Theta, q_u \in [1, q_u^{max}]} & \mathcal{P}(\theta, D_S) - \mathcal{P}(\mathbb{Q}(\theta_u, q_u), D_S) \\ \text{s.t. } & \mathcal{T}(\theta_u, D_S) \leq \mu_u. \end{aligned} \quad (2)$$

where $\mathcal{P}(\theta, D_S)$ is the prediction accuracy of the model θ on the dataset D_S , Θ is the set of generated sub-networks, and q_u^{max} is the maximum number of quantized bits that adhere to the processor's bit-width of device u . For instance, if device u supports 16 bits, the maximum number of quantized bits q_u^{max} is 16. $\mathcal{T}(\theta_u, D_S)$ is the on-device training time of the sub-network θ_u , and μ_u is a threshold, e.g., 10 seconds/local round, predefined by the server for efficient FL. It is worth noting that our sub-network design prioritizes on-device training time over communication time in FL, as training time has a significantly greater impact (as in Tables I-IV).

Selection Process. When a device joins the system, it notifies the server of its resource capabilities. Based on the resource

¹Note that quantization does not affect on-device training time in FedX since quantization will be conducted by the server, as discussed in the FedX training protocol.

Algorithm 1 FedX Training Algorithm

```

1: Inputs:  $N$  devices,  $T$  rounds, quantization function  $\mathbb{Q}$ , server's
   data  $D_S$ , learning rates  $\lambda$  (global) and  $\eta$  (local),  $E$  epochs,
   quantization levels  $\{q_u\}_{u \in [1, N]}$ , devices' local data  $\{D_u\}_{u \in [1, N]}$ 
2: Outputs: Global model  $\theta$ 
3: At the Server:
4:   Initialize global model parameters  $\theta$ 
5:   One-time train the global model parameters  $\theta$  with publicly
   available data at the server  $D_S$ 
6:   Decompose and assign a sub-network  $\{\theta_u^0\}_{u=1}^N$  to every device
    $u$  ( $\theta_u^0 \subset \theta$ ) # Adaptive Model Decomposition in Fig. 2
7:   for  $t = 1, \dots, T$  do
8:     Randomly select a set of devices  $M$ 
9:     for each device  $u$  in  $M$  # in parallel do
10:      Send the quantized sub-network  $\mathbb{Q}(\theta_u^t, q_u)$  to device  $u$  #
        Quantization  $\mathbb{Q}$  in Fig. 2
11:       $\theta_u^{t+1} = \text{LocalTraining}(u, \mathbb{Q}(\theta_u^t, q_u))$  # On-device Training
        in Fig. 2
12:       $\theta \leftarrow \mathcal{G}(\{\theta_u^{t+1}\}_{u \in M})$  # Model Aggregation in Fig. 2
13:      Fine-tune the global model:  $\theta^{t+1} \leftarrow \theta - \lambda \bigtriangledown_{\theta} \mathcal{L}(\theta, D_S)$  #
        Model Fine-tuning in Fig. 2
14:   LocalTraining( $u, \theta_u^t$ ):
15:     Initialize:  $\theta_u^0 \leftarrow \theta_u^t$ 
16:     for  $e = 1, 2, \dots, E$  do
17:        $\theta_u^e = \theta_u^{e-1} - \eta \bigtriangledown_{\theta_u} \mathcal{L}(\theta_u^e, D_u)$ 
18:     Return  $\theta_u^E$ 

```

capabilities of a specific device u , the server can compute the on-device training time and the utility drop using its public data D_S , i.e., using a backup device having the same device type and system resources with u . Our selection process has two steps. First, the server will select all sub-networks with on-device training time less than the threshold μ_u . Second, the server applies a brute-force search to find the optimal combination of a sub-network θ_u among the selected ones in the first step and $q_u \in [1, q_u^{\max}]$, which minimizes the utility drop in Eq. 2. The complexity of this brute-force search selection process is $\mathcal{O}(m \times q)$, where m is the number of sub-networks and q is the number of quantized bits. This search is efficient and effective due to the small search space, allowing for early termination of the search when the utility drops below an acceptable level. Consequently, the server can identify the optimal sub-network θ_u and the number of quantized bits q_u while ensuring efficient on-device training for the device u with the least utility drop.

Notably, optimizing sub-networks is costly and would increase on-device computation and communication during federated training. While joint optimization may yield optimal sub-networks, our approach separates the tasks to reduce costs while maintaining high model utility with limited resources.

B. FedX Training Protocol

Fig. 2 and Alg. 1 present the protocol of FedX training to optimize the objective function in Eq. 1 and its pseudo-code. Initially, the server trains the global model θ on public data D_S , decomposes θ into nested sub-networks θ_u , and then assigns them to devices u based on computational power and processor bit-width. This assignment is performed once.

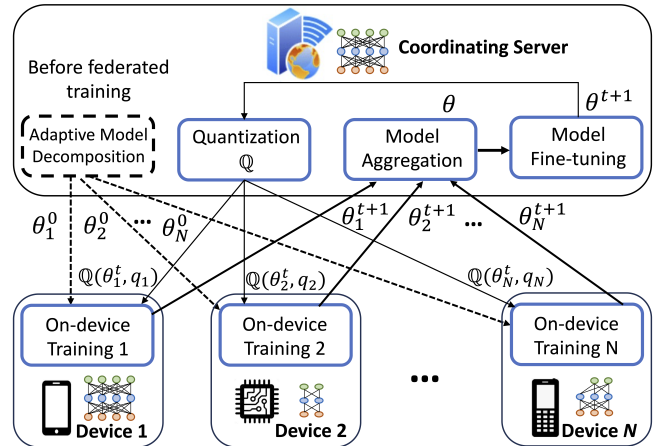


Fig. 2: FedX Training Protocol.

At each iteration t , the server selects a set of M devices and sends different quantized sub-networks $\mathbb{Q}(\theta_u^t, q_u)$ with the numbers of quantized bits $\{q_u\}_{u \in M}$ to each device u in M . The device u uses the quantized sub-network as the local model $\theta_u = \mathbb{Q}(\theta_u^t, q_u)$. Devices independently train and update the local sub-networks θ_u^t using their local data D_u by minimizing the following loss function:

$$\theta_u^{t+1} = \arg \min_{\theta_u} \mathcal{L}(\theta_u, D_u), \quad (3)$$

where $\theta_u = \mathbb{Q}(\theta_u^t, q_u)$. Next, device u sends the updated sub-network θ_u^{t+1} back to the server.

After receiving all the updated sub-networks from the devices $u \in M$, the server aggregates them; that is, multiple sub-networks are updated together into the global model θ . Although other aggregations can be used, we use FedAvg [13] as the aggregation function \mathcal{G} without loss of generality:

$$\theta = \mathcal{G}(\{\theta_u^{t+1}\}_{u \in M}) = (\sum_{u \in M} \theta_u^{t+1}) / \mathbb{H}_M, \quad (4)$$

in which \mathbb{H}_M is a mask with the same size of the global model θ . In \mathbb{H}_M , each value corresponds to the number of devices updating that particular parameter during iteration $t + 1$. For example, in Fig. 1b, all parameters in the sub-network θ_1 (i.e., the gray area) are updated by device 1 tied to θ_1 and device 2 tied to θ_2 . Therefore, the aggregated value of these parameters is $\frac{\theta_1 + \theta_2}{2}$. The additional parameters in θ_2 , which are in θ_1 (i.e., the yellow part), are only updated by θ_2 tied to device 2. Accordingly, their aggregated values are θ_2 .

Then, the server fine-tunes the aggregated global model with its public data D_S by minimizing the loss function:

$$\theta^{t+1} = \arg \min_{\theta} \mathcal{L}(\theta, D_S) + \gamma \|\theta - \mathcal{G}(\{\theta_u^{t+1}\}_{u \in M})\|_2 \quad (5)$$

where γ is a regularization hyper-parameter.

By iteratively minimizing the loss in the devices' local data $\{D_u\}_{u \in [1, N]}$ in Eq. 3 and the loss in the server's publicly available data D_S in Eq. 5, FedX optimizes model utility on both the local and the public datasets.

Regularization as Knowledge Distillation. Adding the regularization term $\|\theta - \mathcal{G}(\{\theta_u^{t+1}\}_{u \in M})\|_2$ into the objective function in Eq. 5 prevents significant shifts between local models trained on devices and the quantized sub-networks optimized using the server’s data. Working as knowledge distillation, this regularization smoothens knowledge sharing across the server and devices in the model update aggregation (Eq. 4), further improving model utility.

After fine-tuning, the server uses the updated global model θ^{t+1} in the next training round.

C. FedX Inference

During inference, each device uses the assigned sub-network that is 1) well-trained on data from the devices and the server and 2) suitable for its computational power and quantization level. In practice, we round up the number of quantized bits to Int8, Float16, and a full precision (Float32) for storing tensors and performing computations on IoT devices.

D. Convergence Analysis

We analyze the convergence rate of FedX when optimizing a strongly convex and Lipschitz continuous loss function $\mathcal{L}(\cdot, \cdot)$ to provide guidelines for practitioners to employ FedX in real-world applications. Our analysis indicates that under the optimization of FedX with a specific learning rate decaying method, the global loss $\mathcal{L}(\theta, D_S)$ will converge with the rate of $\mathcal{O}(\log T/T)$. Moreover, each device receives a sub-network from the converged global model θ^T at the inference time. Therefore, local quantized models will also converge near the global model with a marginal error in the quantization. To derive the analysis, we assume the following:

Assumption 1. $\mathcal{L}(\cdot, \cdot)$ is G -Lipschitz function with respect to θ , i.e., there exists a $G \in \mathbb{R}$ satisfying $\|\mathcal{L}(\theta, \cdot) - \mathcal{L}(\theta', \cdot)\|_2 \leq G\|\theta - \theta'\|, \forall \theta, \theta'$.

Assumption 2. $\mathcal{L}(\cdot, \cdot)$ is a convex function, i.e., $\forall \theta, \theta', w \in [0, 1], \mathcal{L}(w\theta + (1 - w)\theta', \cdot) \leq w\mathcal{L}(\theta, \cdot) + (1 - w)\mathcal{L}(\theta', \cdot)$.

These assumptions are typical in providing convergence analysis for FL algorithms in the previous works [19], [20].

Consider the step $t \in [1, T \times E]$ and denote a device update $v_u^{t+1} = \theta_u^{t+1} - \eta \nabla_{\theta_u^t} \mathcal{L}(\theta_u^t, D_u)$. At step $t : t\%E = 0$, the update of the server is as follows:

$$\theta^t = \theta^{t-1} - \lambda \nabla_{\theta^{t-1}} \mathcal{L}(\theta^{t-1}, D_S) - \lambda \gamma [\theta^{t-1} - \mathcal{G}(v_u^t)],$$

and $\theta^t = \theta^{t-1}$ at step $t : t\%E \neq 0$. Therefore, the server’s updating process is a stochastic gradient descent process of a Lipschitz, convex function $\mathcal{L}(\cdot, \cdot)$. As a result, we can leverage Theorem 2 from Shamir et al. [21] to derive the convergence rate of FedX for the global loss, as follows:

Theorem 1. For a convex function $\mathcal{L}(\theta)$, let $\theta \in \Theta$ such that $\|\Theta\|_2 \leq Q$, $\theta^* = \arg \min_{\theta} \mathcal{L}(\theta)$, and θ^0 is an arbitrary point

in Θ . Consider a stochastic gradient descent with the learning rate $\lambda_t = \frac{Q}{G\sqrt{t}}$. Then for any $T > 1$, the following is true

$$\mathbb{E}(\mathcal{L}(\theta^T, D)) - \mathcal{L}(\theta^*, D) \leq \mathcal{O}\left(\frac{QG \log(T)}{\sqrt{T}}\right). \quad (6)$$

Hence, FedX ensures global model convergence at a rate of $\mathcal{O}(\log(T)/T)$. While local model convergence is hard to quantify due to sub-network decomposition intractability, empirical results show consistent convergence across datasets, highlighting FedX’s optimization efficiency.

IV. EVALUATION

We conduct extensive experiments to explore 1) the interplay among quantized bits, model architectures, and utility, 2) the impact of FedX’s innovative components (i.e., nested sub-networks, quantization selection, and knowledge sharing among the server and devices) on utility, and 3) how FedX saves resources on devices (e.g., CPU and memory), and reduces training, inference, and communication latency.

A. Devices

We test FedX via simulations and an on-device prototype. For simulation, we use a GPU station with 4 NVIDIA GeForce Titan Xp GPUs (12G each), Intel Xeon E5-2637 v4 CPU (3.50GHz), Linux (Ubuntu 16.04), and CUDA 11.3. For on-device prototype, we employ three diverse IoT devices with heterogeneous resources, including 1) *Qualcomm QCS605 AI Kit*, which is equipped with Snapdragon™ QCS605 64-bit ARM v8-compliant octa-core CPU up to 2.5 GHz, Adreno 615 GPU, 8G RAM, and 16 GB eMMC 5.1 onboard storage; 2) *Nvidia Jetson Nano*, which features a quad-core ARM Cortex-A57 CPU with a clock speed of 1.43 GHz and 4 GB RAM; and 3) *Raspberry Pi 5*, which features a quad-core ARM Cortex-A72 CPU with clock speeds of 2.4GHz, and 4GB RAM.

B. Datasets

We conduct experiments on *image classification* using Tiny-ImageNet [22], CIFAR-10 [23], and FEMNIST [24], and on *human activity recognition (HAR)* using the HAR dataset [25]. Tiny-ImageNet, CIFAR-10, FEMNIST, and HAR datasets have 100,000, 50,000, 600,000, and 165,740 training samples, respectively, with corresponding test sets of 10,000, 10,000, 150,000, and 28,770 and class counts of 200, 10, 62, and 5. We simulate 100, 100, 1,000, and 655 devices, respectively. Devices and the server are allocated disjoint training classes with 1) 0–149 (Tiny-ImageNet), 2) 0–7 (CIFAR-10), 3) 0–45 (FEMNIST), and 4) 0–3 (HAR) on devices, and remaining classes at the server. Data is independent and identically distributed (IID) among clients. We also test FedX under non-IID settings with the HAR dataset. Testing includes all classes, highlighting the effectiveness of knowledge sharing in FedX.

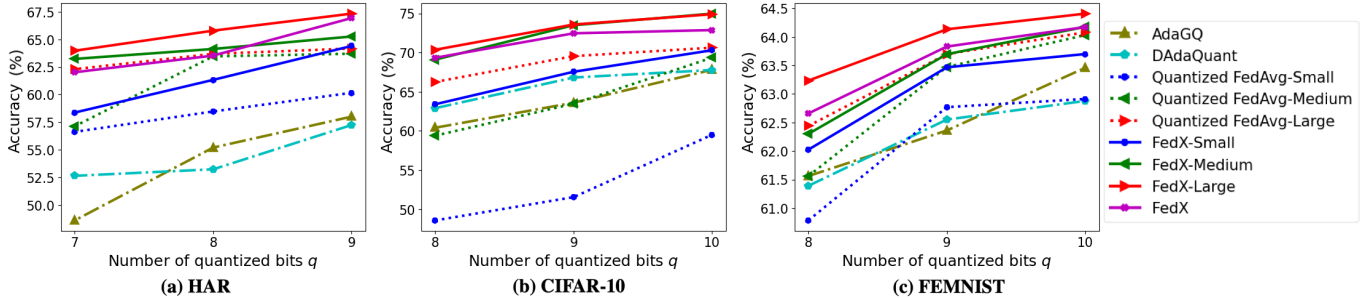


Fig. 3: Model accuracy on the HAR, CIFAR-10, and FEMNIST datasets.

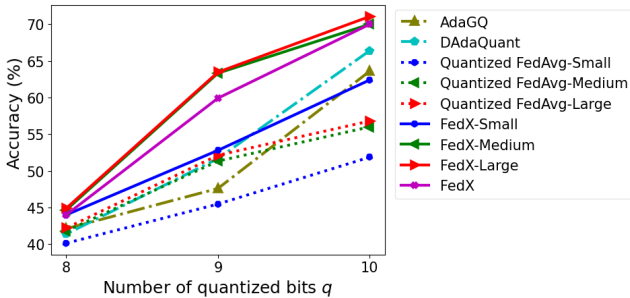


Fig. 4: Model accuracy in the Tiny-ImageNet dataset.

C. Model Architectures

We use MobileNetV3 [16] for image datasets and HAR-Wild [25] for the HAR dataset as global models. The MobileNetV3 model has five CNN blocks with varying layers ($d \in 2, 3, 4$) and channels ($w \in 3, 4, 6$), generating 243 nested sub-networks. To effectively demonstrate the impact stemming from various sub-networks on utility and computation, we examine three sub-networks: **1) small** ($d = 2, w = 3, 2.41\text{M}$ parameters), **2) medium** ($d = 3, w = 4, 3.51\text{M}$ parameters), and **3) large** ($d = 4, w = 6, 6.39\text{M}$ parameters). The HAR-Wild model uses three 1D CNNs with batch norm and five fully connected layers, tailored for mobile devices with low complexity and memory. We create sub-networks by reducing channels from 128 (large) to 64 (medium) and 32 (small), corresponding to 316K, 153K, and 76K parameters, respectively.

To reduce training overhead, we initialize MobileNetV3 pre-trained on ImageNet and HAR-Wild pre-trained on HAR-UCI [26]. FedX training uses a batch size of 32, a learning rate of 0.01 with SGD optimizer, and a regularization rate γ of $1e^{-4}$.

D. Baselines

We evaluate FedX against baselines, i.e., the widely used FedAvg and state-of-the-art quantization-based FL methods for heterogeneous devices, including DAdaQuant [4] and FL AdaGQ [10]. In addition, we compare variants of FedAvg and FedX with different sub-networks and server data availability, including 1) *Quantized FedAvg-Small*: No server data or fine-tuning and all devices use the same small sub-network; 2) *Quantized FedAvg-Medium*: same as 1) but with medium sub-networks; 3) *Quantized FedAvg-Large*: same as 1) but with large sub-networks; 4) *FedX-Small*: Server fine-tunes

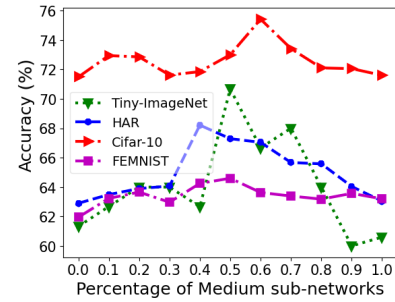


Fig. 5: Varying percentage of medium and small sub-networks.

with data and regularization. All devices use the same small sub-network; 5) *FedX-Medium*: same as 4) but with medium sub-networks; 6) *FedX-Large*: same as 4) but with large sub-networks. Quantization is done at the server in these variants.

In *FedX*, the server has data, fine-tunes with regularization, and performs quantization. To be fair, we evaluate *FedX*, *FedAvg*, and variants with *DAdaQuant* and *AdaGQ*, where the server has data, fine-tunes without regularization, and quantization occurs on devices as in their conventional settings.

Model Accuracy. To evaluate model utility, we compute the average accuracy across devices using their testing data, as follows: $Acc = \frac{1}{N} \sum_{u \in [1, N]} \left[\frac{1}{|D_u^{test}|} \sum_{x \in D_u^{test}} \mathbb{I}(\theta_u(x), y) \right]$, where $\mathbb{I}(\theta_u(x), y) = 1$ if $\theta_u(x) = y$ and 0 otherwise. D_u^{test} consists of testing samples and its size $|D_u^{test}|$ at the device u .

E. Model Utility Evaluation

Fig. 4 illustrates model utility on the Tiny-ImageNet dataset across numbers of quantized bits, and different FedX and baseline versions. Overall, FedX-Medium and FedX-Large perform the best. FedX achieves a better balance between sub-network sizes and the numbers of quantized bits. Large sub-networks do not consistently lead to a notable accuracy improvement. There is a marginal difference in model accuracy between FedX-Medium and FedX-Large across numbers of quantized bits. However, using a sub-network that is too small would significantly damage the model utility, i.e., FedX-Small. This illustrates a non-trivial trade-off between sub-network sizes and the number of quantized bits in FL. FedX mitigates this problem by identifying the most suitable sub-network and quantized bits for each device, minimizing performance degradation while adhering to the device's resource constraints.

TABLE I: FedX Training on Qualcomm AI Kit.

Dataset	Model Size	CPU (%)	RAM (MB)	Training time (s)	Communication time (s)
Tiny-ImageNet	Small	41.4	922.4	34.9	2.29
	Medium	44.8	2005.7	57.3	2.96
	Large	45.5	2139.9	77.5	3.44
CIFAR10	Small	35.3	1072.4	24.3	2.05
	Medium	36.5	1197.5	38.0	2.69
	Large	36.8	1322.7	49.8	3.17
FEMNIST	Small	35.8	478.4	24.3	2.13
	Medium	36.4	761.9	37.5	2.77
	Large	36.9	920.8	49.9	3.25
HAR	Small	31.6	232.9	2.6	0.01
	Medium	47.2	245.4	2.8	0.04
	Large	52.8	252.1	4.4	0.13

Given the marginal accuracy gap between FedX-Medium and FedX-Large, but a significant gap with FedX-Small, for the following experiments, we use only the *medium and small sub-networks* in FedX. In this setup, half of the devices use the same small sub-network and half uses the medium one. We change this proportion in our ablation study to understand the trade-off between nested sub-networks and quantization selection. DAdaQuant and AdaGQ also use two sub-networks for a fair comparison. As shown in Fig. 4, FedX outperforms DAdaQuant and AdaGQ in terms of model utility, with average improvements of 2.28-3.01%, 8.20-12.28%, and 1.9-4.76%, when the number of quantized bits increases from 8 to 10. Also, FedX outperforms the most accurate Quantized FedAvg-Large by 2.19%, 2.49%, and 11.56% with 8, 9, and 10 quantized bits, respectively. This gain stems from nested sub-networks and an efficient training algorithm that boosts knowledge transfer and reduces device quantization costs, enhancing performance.

We observe similar trends with HAR, CIFAR-10, and FEMNIST datasets (Fig. 3), where FedX-Medium and FedX-Large outperform the baselines, demonstrating FedX’s generalization across datasets and models. These results are from real-world data, considering heterogeneous quantization, limited resources, and data distribution differences, with only a 3.6% drop compared to homogeneous devices without constraints [25].

F. Ablation Study

To comprehensively examine the effects of FedX’s innovative components, we conduct ablation studies on 1) the trade-off between nested sub-networks and quantization selection by varying the percentages of different types of sub-networks and quantization levels, 2) the effects of knowledge-sharing among the server and devices, with and without regularization.

Nested Sub-networks and Quantization Selection. We vary the percentage of clients with medium sub-networks in FedX from 0% to 100%, using smaller quantization levels (i.e., 9 for CIFAR-10, FEMNIST, Tiny-ImageNet; 8 for HAR) for medium sub-networks and larger levels (11 and 10, respectively) for small sub-networks. Given different percentages and datasets, model utility typically peaks when 40 – 60% of medium sub-network clients are used, achieving 70.67%, 68.21%, 75.41%, and 64.60% on Tiny-ImageNet, HAR, CIFAR-10, and FEMNIST (Fig. 5). Model utility drops by 2.05% – 5.31% at

TABLE II: FedX Training on Raspberry Pi 5.

Dataset	Model Size	CPU (%)	RAM (MB)	Training time (s)	Communication time (s)
Tiny-ImageNet	Small	93.6	479.5	17.6	2.29
	Medium	92.6	576.8	32.1	2.96
	Large	91.9	696.2	43.4	3.44
CIFAR10	Small	89.3	638.9	7.5	2.05
	Medium	90.6	632.2	11.6	2.69
	Large	90.6	632.9	14.5	3.17
FEMNIST	Small	87.3	368.5	7.5	2.13
	Medium	88.8	418.6	11.1	2.77
	Large	89.9	418.7	13.7	3.25
HAR	Small	79.8	279.0	0.4	0.01
	Medium	84.8	287.0	1.2	0.04
	Large	83.4	296.8	2.7	0.13

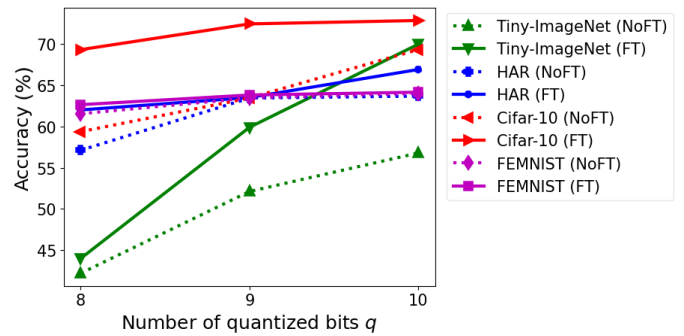


Fig. 6: FedX with and without Fine-tuning (FT and NoFT). higher percentages (i.e., more clients) of medium sub-network clients with smaller quantization levels. These observations highlight the need to balance sub-network sizes and quantization for optimal performance and memory efficiency.

Knowledge Sharing via Regularization. We compare models with and without fine-tuning, reflecting the presence or absence of knowledge sharing among the server and devices. Fig. 6 shows consistently higher model utility with server fine-tuning. This is because when the server and the devices have different class distributions, the fine-tuning process fosters knowledge sharing among them, boosting FedX performance.

Non-IID Settings. We conduct experiments using the HAR dataset, where the number of samples per class per device follows an α -symmetrical Dirichlet distribution and $\alpha \in [0.01, 1, 100]$. FedX achieves 79.96% accuracy when the data is extremely diverse (i.e., the concentration parameter $\alpha = 0.01$), compared with 68.21% in the IID setting. This utility improvement is because each device has fewer classes resulting in better local minima for their models. We observe a similar trend with different levels of non-IID, i.e., $\alpha \in [1, 100]$.

G. System Performance

On-device Training. The experiments are conducted over small, medium, and large sub-networks across datasets. We train on 750 samples with a batch size of 32 (i.e., one training round) and report the mean of 20 measurements in each dataset.

Tables I, II, and III show the FedX resource consumption, training, and communication times across devices and datasets.

TABLE III: FedX Training on Nvidia Jetson Nano.

Dataset	Model Size	CPU Training				GPU Training				Communication time (s)		
		CPU (%)	CPU RAM (MB)	CPU Power (MW)	Training time (s)	GPU (%)	GPU RAM (MB)	GPU Power (MW)	CPU RAM (MB)			
Tiny-ImageNet	Small	92.6	98.4	2267	122.4	99.7	579	1275	616	687	4.6	2.29
	Medium	93.6	129	2375	216.3	99.7	687	1338	611	663	6.9	2.96
	Large	97.9	151	2370	241.6	99.6	755	1450	530	885	16.9	3.44
CIFAR10	Small	90.1	141	1914	87.4	99.7	511	722	597	788	5.6	2.05
	Medium	90.8	144	1781	189.1	99.7	549	1057	604	900	8.5	2.69
	Large	82.3	144	1800	241.3	99.7	573	943	583	909	20.2	3.17
FEMNIST	Small	92.4	72.9	1933	90.6	99.7	509	1071	629	850	5.3	2.13
	Medium	92.8	79.5	2014	173.9	99.0	527	886	628	851	8.0	2.77
	Large	92.1	86.2	2020	233.6	99.7	561	1006	616	917	18.9	3.25
HAR	Small	88.8	65.2	1307	2.8	52.1	474	287	665	828	0.5	0.01
	Medium	92.7	67.2	2371	2.7	85.5	478	647	662	672	0.9	0.04
	Large	91.9	73.0	2364	6.5	99.7	520	1450	660	783	0.8	0.13

Dataset	Mechanism	On-device computation time (s)	Communication time (s)	Server quantization time (s)	Aggregation time (s)	Fine-tuning time (s)	Total time (s)
Tiny-ImageNet	DAdaQuant	112.4	1.23	N/A	0.032	5.07	118.73
	AdaGQ	112.4	1.72		0.032	N/A	114.15
	Quantized FedAvg	77.5	3.44		0.032	N/A	95.5
CIFAR10	DAdaQuant	74.3	1.13	N/A	0.032	4.11	79.57
	AdaGQ	74.3	1.59		0.032	N/A	75.92
	Quantized FedAvg	49.8	3.17		0.032	N/A	62.6
FEMNIST	DAdaQuant	75.0	1.16	N/A	0.033	3.73	79.92
	AdaGQ	75.0	1.63		0.033	N/A	76.66
	Quantized FedAvg	49.9	3.25		0.033	N/A	61.2
HAR	DAdaQuant	5.7	0.05	N/A	0.031	0.47	6.25
	AdaGQ	5.7	0.07		0.031	N/A	5.80
	Quantized FedAvg	4.4	0.13		0.031	N/A	8.67
	FedX	4.4	0.13		2.78	0.031	7.81

TABLE IV: End-to-end Operation Time.

Training times range from 0.5 to 77.5 seconds (s), while communication times (i.e., the round-trip time of sending and receiving sub-networks with the network bandwidth of 30 mbps) span 0.01s to 3.44s. These training and communication times are fast and practical. In addition, CPU usage during training ranges from 31.6% to 97.9%, with maximum RAM usage from 65.2 MB to 2,139.9 MB, indicating on-device training feasibility. Notably, GPU training on Nvidia Jetson Nano via CUDA uses comparable power as CPU, but it is 3 to 31× faster than CPU training, especially for larger datasets and models (i.e., 14 to 31 × for Tiny-ImageNet compared to 3 to 8 × for HAR), highlighting FedX’s efficiency with growing GPU adoption in IoT devices. This observation highlights FedX’s efficiency with growing GPU adoption in IoT devices.

On-device Inference. Since FedX supports Int8, Float16, and Float32, we report the inference time using the maximum supported bits. Fig. 7 shows the times on the Qualcomm AI Kit across sub-networks and quantized bits. While the small HAR model shows negligible differences, other models benefit from Int8 and Float16, reducing latency. For Tiny-ImageNet, Int8 and Float16 small sub-networks take 0.13s compared to 0.16s for Float32. Medium and large Int8 sub-networks take 0.19s and 0.27s, with Float16 slightly higher. Overall, the inference time is under 0.3s, showing FedX’s efficiency and feasibility.

End-to-end Operation Time. FedX’s end-to-end operation includes on-device computation, communication, quantization,

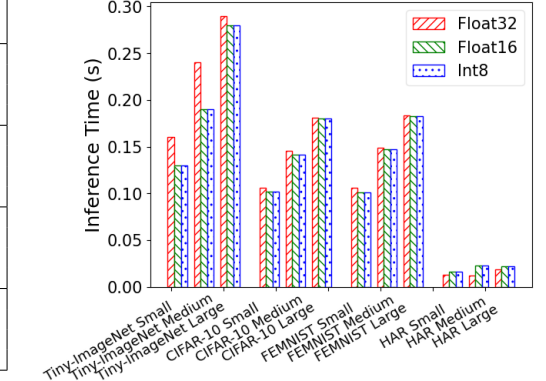


Fig. 7: FedX’s On-device Inference time.

aggregation, and fine-tuning. Table IV shows the average operation time over 20 rounds. Since the devices run in parallel, on-device computation and communication are measured by the largest sub-network on Qualcomm AI Kit, which is the slowest among the IoT devices. For a fair comparison, we evaluate DAdaQuant, AdaGQ, and Quantized FedAvg with the large sub-network, as it offers the highest accuracy and these methods do not vary model sizes.

DAdaQuant and AdaGQ have on-device computation overhead from on-device quantization, causing on-device computation times from 30% to 49% longer than in FedX and Quantized FedAvg-Large. In FedX, the quantization time is between 3.63 and 2.78s per round, making it 3.51×, 2.20×, 2.22×, and 1.48× faster than Quantized FedAvg-Large in the Tiny-ImageNet, CIFAR-10, FEMNIST, and HAR datasets, respectively. The server consumes a negligible aggregation time, lasting about 0.03s. For fine-tuning, the time for DAdaQuant and FedX is measured by training the same sample size across datasets, while Quantized FedAvg-Large does not perform fine-tuning after quantization.

The total operation time on the HAR dataset is negligible due to HAR-Wild model’s small number of parameters. In other datasets, FedX is faster than DAdaQuant by 22.7% to 24.3%, AdaGQ by 19.0% to 21.1%, and Quantized FedAvg-Large by 1.1% to 5.5%, even though Quantized FedAvg-Large does not fine-tune after quantization. FedX works efficiently on-device, enhances

end-to-end operation, and offers a more practical FL system.

More importantly, FedX converges faster than the baselines due to enhanced knowledge sharing between the server and devices. For example, in the Tiny-ImageNet, FedX, FedAvg, DAdaQuant, and AdaGQ require 6, 15, 32, and 30 rounds to converge. This result is significant as FedX reduces training times per round and minimizes the number of training rounds.

Remark. FedX offers four key advantages: **(1)** FedX has higher model utility, with a lower resource consumption and quantization time. **(2)** FedX’s quantization is $3.51 \times$ to $8.43 \times$ faster than FedAvg, DAdaQuant, and AdaGQ. **(3)** Thanks to knowledge sharing between the server and devices, FedX converges quickly. **(4)** With the on-device training time under 77.5s, on-device inference time under 0.3s, and communication time under 3.44s, FedX is feasible in real-world applications.

V. RELATED WORK

Device heterogeneity poses a key challenge in FL, with solutions like dropping or partial updates leading to resource waste and utility drop [27], [28]. Two main approaches aim to tackle this challenge and improving communication efficiency.

First, compression methods, such as quantization, pruning, sparsification, and sampling [6], [29]–[33], reduce the amount of data transfers but may impact utility or increase computational overhead. In contrast, FedX improves utility and reduces overhead with server-side quantization and knowledge transfer.

Second, knowledge distillation (KD) transfers knowledge from large to smaller models without sacrificing utility [8], [34]–[38]. Two main approaches are 1) data-additional KD, combining public and private data for training, and 2) data-free KD, transmitting prediction scores without public data. In FedX, we employ quantization and knowledge transfer, to improve knowledge sharing while reducing overhead.

Using FL in IoT devices poses challenges in terms of communication efficiency and heterogeneity. Proposed solutions include codistillation that exchanges model predictions to train local models, device-inclusion that assigns models based on resource capabilities, and device selection using resource-based criteria [39]–[41]. However, they lack adaptive quantization to balance communication, computation, and utility.

VI. CONCLUSION

This paper presented FedX, a novel FL system with adaptive model decomposition and quantization for heterogeneous IoT devices. FedX assigns smaller sub-networks with higher quantization to resource-limited devices and larger ones with lower quantization to resource-rich devices, enhancing knowledge sharing and resource efficiency. Knowledge sharing occurs by aggregating nested sub-networks through the global model each round. Optimized and diverse sub-network sizes significantly reduce computational overhead compared to single large models. FedX ensures global model convergence. Overall, FedX improves utility and system effectiveness while reducing training, quantization, and inference overhead, making it suitable for heterogeneous IoT environments.

ACKNOWLEDGMENTS

This research was supported in part by the National Science Foundation (NSF) under Grants No. CNS 2237328, DGE 2043104, and CNS-1935928.

REFERENCES

- [1] K. Bonawitz *et al.*, “Towards FL at scale: System design,” *MLSys*, 2019.
- [2] T. Wang *et al.*, “Applications of FL in mobile health: Scoping review,” *JMIR*, 2023.
- [3] A. T. Thorgerisson *et al.*, “Probabilistic prediction of energy demand and driving range for electric vehicles with federated learning,” *IEEE OJVT*, 2021.
- [4] R. Höning, Y. Zhao, and R. Mullins, “Dadaquant: Doubly-adaptive quantization for communication-efficient federated learning,” in *ICML*, 2022, pp. 8852–8866.
- [5] Y. Oh *et al.*, “Fedvqcs: FL via vector quantized compressed sensing,” *TWC*, 2023.
- [6] J. Hamer, M. Mohri, and A. T. Suresh, “Fedboost: A communication-efficient algorithm for federated learning,” in *ICML*, 2020.
- [7] Z. Jiang, Y. Xu, H. Xu, Z. Wang, J. Liu, Q. Chen, and C. Qiao, “Computation and communication efficient FL with adaptive model pruning,” *IEEE TMC*, 2023.
- [8] D. Li and J. Wang, “Fedmd: Heterogenous federated learning via model distillation,” *NeurIPS Workshop*, 2019.
- [9] L. Li *et al.*, “To talk or to work: Flexible communication compression for energy efficient FL over heterogeneous mobile edge devices,” in *IEEE INFOCOM*, 2021.
- [10] H. Liu *et al.*, “Communication-efficient federated learning for heterogeneous edge devices based on adaptive gradient quantization,” in *INFOCOM*, 2023.
- [11] S. M. S. Mohammadabadi, S. Zawad, F. Yan, and L. Yang, “Speed up federated learning in heterogeneous environment: A dynamic tiering approach,” *arXiv*, 2023.
- [12] Z. Zhang, A. Pinto, V. Turina, F. Esposito, and I. Matta, “Privacy and efficiency of communications in federated split learning,” *IEEE Transactions on Big Data*, 2023.
- [13] P. Kairouz *et al.*, “Advances and open problems in FL,” *Found. Trends ML*, 2021.
- [14] D. Alistarh, D. Grubic, J. Li, R. Tomioka, and M. Vojnovic, “Qsgd: Communication-efficient sgd via gradient quantization and encoding,” *NeurIPS*, vol. 30, 2017.
- [15] M. Sahni, S. Varshini, A. Khare, and A. Tumanov, “Compofa: Compound once-for-all networks for faster multi-platform deployment,” *ICLR*, 2021.
- [16] A. Howard *et al.*, “Searching for mobilenetv3,” in *ICCV*, 2019.
- [17] W. Jiang *et al.*, “Accuracy vs. efficiency: Achieving both through fpga-implementation aware neural architecture search,” in *DAC*, 2019.
- [18] H. Cai, C. Gan, T. Wang, Z. Zhang, and S. Han, “Once-for-all: Train one network and specialize it for efficient deployment,” *ICLR*, 2020.
- [19] X. Li, K. Huang *et al.*, “On the convergence of fedavg on non-iid data,” 2020.
- [20] X. Wu, F. Huang *et al.*, “Faster adaptive federated learning,” in *AAAI*, 2023.
- [21] O. Shamir and T. Zhang, “Stochastic gradient descent for non-smooth optimization: Convergence results and optimal averaging schemes,” in *ICML*, 2013, pp. 71–79.
- [22] Y. Le and X. Yang, “Tiny imagenet visual recognition challenge,” *CS 231N*, 2015.
- [23] A. Krizhevsky *et al.*, “Learning multiple layers of features from tiny images,” 2009.
- [24] S. Caldas *et al.*, “Leaf: A benchmark for federated settings,” *NeurIPS*, 2019.
- [25] X. Jiang *et al.*, “Flsys: Toward an open ecosystem for FL mobile apps,” *TMC*, 2022.
- [26] D. Anguita, A. Ghio, L. Oneto *et al.*, “Human activity recognition on smartphones using a multiclass hardware-friendly support vector machine,” 2012.
- [27] Z. Chai *et al.*, “Tiff: A tier-based federated learning system,” in *ACM HPDC*, 2020.
- [28] T. Zhang, L. Gao, S. Lee, M. Zhang, and S. Avestimehr, “Timelyfl: Heterogeneity-aware asynchronous FL with adaptive partial training,” in *CVPR*, 2023.
- [29] N. Shlezinger *et al.*, “Uveqfed: Universal vector quantization for FL,” *TSP*, 2020.
- [30] Z. Zhang, Z. Tianqing, W. Ren, P. Xiong, and R. Choo, “Preserving data privacy in federated learning through large gradient pruning,” *Computers & Security*, 2023.
- [31] X. Jiang and C. Borcea, “Complement sparsification: Low-overhead model pruning for federated learning,” *AAAI*, 2023.
- [32] A. Abdi and F. Fekri, “Quantized compressive sampling of stochastic gradients for efficient communication in distributed deep learning,” 2020, pp. 3105–3112.
- [33] S. Vithana and S. Ulukus, “Model segmentation for storage efficient private federated learning with top r sparsification,” in *CISS*, 2023.
- [34] J. Zhang, S. Guo, J. Guo, D. Zeng, J. Zhou *et al.*, “Towards data-independent knowledge transfer in model-heterogeneous FL,” *IEEE Trans. Comput.*, 2023.
- [35] Z. Zhu, J. Hong, and J. Zhou, “Data-free knowledge distillation for heterogeneous federated learning,” in *ICML*, 2021.
- [36] C. Wu, F. Wu, L. Lyu, Y. Huang, and X. Xie, “Communication-efficient federated learning via knowledge distillation,” *Nature communications*, p. 2032, 2022.
- [37] Y. Chen, W. Lu, X. Qin, J. Wang, and X. Xie, “Metafed: Federated learning among federations with cyclic knowledge distillation for personalized healthcare,” *IEEE Transactions on Neural Networks and Learning Systems*, 2023.
- [38] Y. Xu and H. Fan, “Feddk: Improving cyclic knowledge distillation for personalized healthcare federated learning,” *IEEE Access*, 2023.
- [39] S. Sodhani, O. Delalleau, M. Assran, K. Sinha, N. Ballas, and M. Rabbat, “A closer look at codistillation for distributed training,” *arXiv*, 2020.
- [40] Y. Cho, J. Wang, T. Chirvolu, and G. Joshi, “Communication-efficient and model-heterogeneous personalized FL via clustered knowledge transfer,” *J-STSP*, 2023.
- [41] L. Fu, H. Zhang, G. Gao, M. Zhang, and X. Liu, “Client selection in federated learning: Principles, challenges, and opportunities,” *IEEE IoT-J*, 2023.